Cement and Concrete Composites 73 (2016) 289–298

Contents lists available at ScienceDirect

Cement and Concrete Composites

journal homepage: www.elsevier.com/locate/cemconcomp

Mechanical properties of ultra-lightweight cement composite at low temperatures of 0 to −60 °C

Xuemei Liu [a, *], Min-Hong Zhang [b], Kok Seng Chia [c], Jiabao Yan [d], J.Y. Richard Liew [b]

[a] School of Civil Engineering and Built Environment, Queensland University of Technology (QUT), Australia
[b] Department of Civil and Environmental Engineering, National University of Singapore, Singapore
[c] NauticAWT Ltd, Singapore
[d] Department of Civil Engineering, Tianjin University, China

ARTICLE INFO

Article history:
Received 7 November 2014
Received in revised form
28 August 2015
Accepted 18 May 2016
Available online 10 August 2016

Keywords:
Ultra-lightweight cement composite
Concrete
Arctic offshore structure
Stress
Strain
Strength
Low temperature

ABSTRACT

This paper presents an experimental study on mechanical properties of an innovative ultra-lightweight cement composite (ULCC) at low temperatures down to −60 °C in comparison with those at ambient temperature. Those properties include stress-strain curve, ultimate strength, elastic modulus, Poisson ratio, and flexural tensile behavior. Effect of curing condition is also evaluated. In addition, the performance of the ULCC is compared with that of a normal weight concrete (NWC) and a lightweight concrete (LWC) with similar 28-day compressive strength. The cylindrical compressive strength of the NWC and LWC was increased generally with the reduction in temperature. However, the same phenomenon was not observed for the ULCC. The elastic modulus of the ULCC did not change much, whereas the elastic modulus of the NWC increased significantly with the reduction of temperature from 30 °C to −60 °C. Strain of the ULCC at the peak load was generally much higher than that of the NWC and LWC, and was generally not affected by the temperature. The flexural strength of the three concretes was increased with the reduction in temperature. Duration of the moist curing did not affect the performance of the ULCC under compression significantly, but influenced its flexural strength significantly.

1. Introduction

After the discovery of oil and gas reservoirs in the Arctic region in the last century, productions and explorations continue to this day, contributing to the growth of oil and gas industry. A type of ultra lightweight cement composite (ULCC) was developed [9] to tailor the offshore structural applications in the Arctic areas, in particular for offshore floating structures and liquefied natural gas (LNG) storage tanks. For floating structures, it is desirable that these structures are of low self-weight. In construction of offshore structures such as oil platforms, most base structures are floated out to sites by tugboats and then completed on site. The low self-weight improves deployment and on-site installation of the structures. The ULCC generally has a unit weight of at least 40% less than that of conventional concrete and compressive strength of up to about 65 MPa with low permeability [23]. The ULCC has lower densities and higher specific strengths (compressive strength/density) compared with lightweight concrete (LWC). In addition, the permeability of ULCC is significantly lower than that of the LWC [22,23]. Thus, the ULCC is more suitable for floating structures in offshore environment with potentially reduced maintenance costs due to reduced permeability.

According to Danish Meteorological Institute (Dmi) Centre for Ocean and Ice, the daily mean temperatures for the Arctic area north of the 80th parallel ranged from - 40 °C to 2 °C from the period of 1958–2014 [13]. This raises the question about the possibility of using the ULCC in such environments, since low temperatures could affect the mechanical properties of the ULCC as a structural material and in steel-ULCC composite structural members. However, no information on the mechanical properties of the ULCC under subzero temperatures of 0 to −60 °C is currently available. This initiates the research described in this paper.

For normal weight concrete (NWC), mechanical properties of the concrete are improved when concrete is cooled down to subzero temperatures [21,24,27,31,34]. Compressive strength, modulus of elasticity, Poisson's ratio, tensile strength, and flexural strength of concrete generally increase with decreasing temperature (below 0 °C). The aforementioned improvements are attributed to the

* Corresponding author.
E-mail address: x51.liu@qut.edu.au (X. Liu).

http://dx.doi.org/10.1016/j.cemconcomp.2016.05.014
0958-9465/

freezing of water and formation of ice in pores and microcracks inside the concrete. Therefore, the behavior of concrete at low temperatures is governed by moisture content in pores and freezing temperature of pore solution. It was found, for example, that dry concrete is little affected by such low temperature and not much affected at 50% RH [24]. Miura [29] found that the increase in the compressive strength is nearly proportional to the moisture content of the NWC, and a relationship between the compressive strength and the moisture content and low temperature was proposed.

When concrete is cooled to 0 °C, most of the water in the concrete does not freeze immediately. The freezing point of water in capillary pores is affected by the pore size and salt concentration in pores. Lower temperatures are required to freeze water in smaller pores or in pores with salt solutions. Skapski et al. [35] presented an equation [Eq (1)] that co-relates the ice crystal radius (γ) which is assumed to be close to the true pore radius (γ_p) to temperature (T) at which water freezes, and the relationship is illustrated in Fig. 1.

$$T = \frac{-2T_m\gamma_{iw}}{H_f\gamma\rho_i} \quad (1)$$

Where $T_m = 273$ K (0 °C)

γ_{iw} = surface tension between water and ice (0.031 N/m)
H_f = normal heat of fusion (333,000 J/kg)
γ = ice crystal radius (m)
ρ_i = density of ice (917 kg/m^3).

The true radius of the pore γ_p, (in m) can be calculated with the following equation according to [16].

$$\gamma_p = \gamma + 12.4 \times 10^{-10}\,(\text{m}) \quad (2)$$

With prediction based on the above equations without considering the salt concentration in the pore solution, water in large capillary pores with diameter of 50 nm could be frozen when the temperature drops to -2 °C and water in medium capillary pores with diameter of 10 nm would most probably be frozen when the temperature drops down to about −7 °C.

With the increase in the salt concentration the freezing temperature decreases. The presence of salt in pore water may result in a further reduction in the freezing temperature within the order of another 1 °C [28].

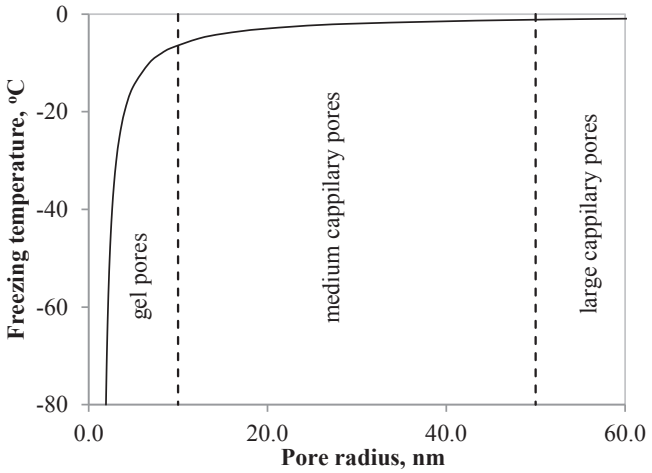

Fig. 1. Freezing temperature as a function of pore size.

This research project aims to investigate mechanical performance of the ULCC at low temperatures down to −60 °C in comparison with that obtained at ambient temperature of about 30 °C. This ambient temperature was used since experiments were conducted in Singapore, a tropical country. The mechanical behaviors investigated include stress-strain curve, ultimate strength, elastic modulus, Poisson ratio when subjected to uni-axial compressive loading, and flexural tensile behavior. Effect of curing condition on the behavior of the ULCC is also evaluated. In addition, the performance of the ULCC is compared with that of a NWC and a LWC with similar 28-day compressive strength at the ambient temperature of 30 °C.

2. Experimental details

2.1. Test specimens

2.1.1. Mix proportions

Mix proportions of the ULCC, NWC, and LWC are presented in Table 1. The ULCC had a w/b of 0.35, and contained 5% silica fume by mass of cementitious materials and 0.5% polyvinyl alcohol (PVA) fibers by volume of the ULCC. To achieve comparable 28-day strength, the NWC had a w/b of 0.45 without using silica fume. The LWC had the same w/b as that of the ULCC and silica fume was also incorporated to achieve the design strength.

ASTM Type 1 Portland cement (also complying with [5] for CEM I 52.5N) was used for all the mixtures. The silica fume was undensified with 95.9% of SiO_2 and a specific surface area of 21.3 m^2/g.

Commercially available cenospheres were used as “micro” aggregate to achieve low unit weight of the ULCC. They were hollow spheres extracted from fly ash generated from coal-burning power plants. The cenospheres generally have hollow interior covered by a thin shell with thickness about 5–10% of its diameter [8]. Due to the hollow structure, cenospheres have low particle densities. The cenospheres used in this study had an average particle density of about 860 kg/m^3 with particle sizes ranging from 100 to 300 μm. The cenospheres had low CaO content of less than 1% but high sum of SiO_2 and Al_2O_3 contents of approximately 90% with great amounts of amorphous materials. Since cenospheres are derived from fly ash of coal-burning power plants, they contain amorphous silica and have pozzolanic reactivity as fly ash. However, their relatively large sizes up to several hundred microns suggest that the pozzolanic reactivity of the cenospheres might be limited at ambient temperatures. Due to the sizes and amorphous silica in the cenospheres, there is a concern of long-term durability of lightweight cement composites due to possible alkali–silica reactivity (ASR) of the cenospheres. Although this durability problem generally occurs in concretes/mortars containing aggregates with reactive silica, it was reported that undispersed silica fume agglomerates might act as “reactive aggregates” and cause similar durability problem [18,25]. Research by Ref. [36] shows that the cenospheres are not deleterious to the concrete from this perspective.

Natural sand and crushed granite with a maximum nominal size of 20 mm were used for the NWC. These aggregates satisfied the grading requirements of ASTM C33, and had specific gravities of 2.60 and 2.65, respectively. A commercially available expanded clay type lightweight aggregate (LWA) with sizes of 4–8 mm and natural sand were used for the LWC. The LWA had a particle density of 1200 kg/m^3 and 1-hr water absorption of 9%.

A polycarboxylate-based superplasticizer was used for all the mixtures to obtain workable fresh concretes. A commercially available shrinkage reducing admixture (SRA) based on glycol derivative was used in the ULCC to reduce shrinkage.

Table 1
Mix proportion of concrete mixtures.

Mix ID	W/b	Water	Cement	SF	Cenospheres	Sand	Coarse aggregate	SP	SRA	PVA fibers
		kg/m^3						L/m^3	L/m^3	% By concrete volume
ULCC	0.35	265	775	41	335	–	–	5.5	20.8	0.5
NWC	0.45	186	414	–	–	651	1064	1.4	0	0
LWC	0.35	175	460	40	–	793	409 (LWA)	3.0	0	0

Polyvinyl alcohol (PVA) fibers with a length of 6 mm and a diameter of 27 μm were used in the ULCC to reduce its brittleness. The fibres had a tensile strength of 1600 MPa, an elastic modulus of 39 GPa, a maximum elongation of 7%, and a specific gravity of 1.30.

2.1.2. Specimen preparation and curing

Specimens used for various tests are described in Table 2. Cubes of 100-mm were used for determining the density and compressive strength. Cylinders of 100 × 200-mm were used for determining the compressive behavior of concretes at various temperatures except for the ULCC. After conducting the low temperature test on NWC, it was found that the maximum stress of the NWC at −60 °C exceeded the capacity of the equipment. With the consideration of the possible increased ultimate load of ULCC at −60 °C and the limitations of the loading capacity of the testing equipment, smaller cylinders of 75 × 150-mm were used for the ULCC, considering the ULCC containing no coarse aggregate. It is recognized that sizes of the specimens have effect on the strengths of the concrete. However, based on compressive strength data from literature within the 20–60 MPa range analyzed by Ref. [11]; the mean strength ratio of S75/S150 (strength determined with Ø75 × 150-mm cylinders/ strength determined with Ø150 × 300-mm cylinders) is within 0.98–1.04. It can be deduced that the difference between the mean compressive strength determined with Ø75 × 150-mm cylinders and that with Ø100 × 200-mm specimens would not be significant. Prisms of 102 × 76 × 402-mm were used for determining the behavior of the concretes subjected to bending.

For the ULCC, the cement, silica fume, and cenospheres were first dry-mixed in an 80-L pan mixer for about 1 min before water and superplsticizer were added and mixed at an ambient temperature of 30 °C. When a homogeneous mixture was obtained with suitable workability, usually about 5 min after adding the water and superplasticizer, the fibres were added and the mixing continued for another 5 min.

The NWC and LWC were also mixed in the pan mixer. The LWA was pre-soaked in water for 1 h before being mixed in concrete. Water in excess of the amount required for the aggregate absorption and concrete mixing was used in order to ensure that all the aggregate particles were fully submerged during soaking. After 1 h the excess water was removed and the mass added into the mixer included that of oven-dried aggregate, water absorbed in 1 h and mixing water based on concrete mix proportion (Table 1). Prior to the soaking/mixing, all LWA was oven dried and cooled down to ambient temperature.

The resulting mixture was sampled to determine the workability in terms of flow consistency for the ULCC and slump for the NWC and LWC. After that, the specimens described in Table 2 were prepared and consolidated on a vibration table. The molded specimens were covered with wet cloths and protected from moisture loss with a plastic sheet. The NWC and LWC specimens were de-molded after 24 h and moist-cured in a fog room for 7 days, followed by exposure to laboratory air for 21 days (temperature about 30 °C). The ULCC specimens were de-molded about 48 h after casting due to the retarding effect from the SRA.

To investigate the effect of curing and moisture conditions on various properties under low temperatures, two series of ULCC specimens were prepared. One series had similar curing to that of NWC and LWC, and was denoted as ULCC(D), Whereas the other series was cured in the fog room after demoding at relative humidity of >95% and temperature of 28±1 °C until 28 days, and was denoted as ULCC(S).

2.2. Tests

The mechanical performance of the concretes, including the stress-strain relationship, compressive strength, flexural tensile strength, elastic modulus, and Poisson's ratio was determined at ambient temperature of about 30 °C and low temperatures of 0 to −60 °C. Since the performance is affected by ice formed in pores, water accessible porosity of the concretes was also determined.

Table 2
List of material properties evaluated and relevant test methods.

Property determined	Standard	Concrete type & specimen sizes	Curing conditions	Testing age	Number of specimens
Flow consistency	BS EN 1015 −3:1999	ULCC	ULCC(S): 28-d moist curing ULCC(D), NWC, & LWC:	Fresh	–
Slump test	BS EN 12350−2: 2009	NWC & LWC	7-d moist curing + 21-d lab air exposure		–
Density of hardened specimens	BS EN 12390 −7:2009	100-mm cube		7 & 28 days	3 for each test
Compressive strength	BS EN 12390 −3:2009	100-mm cube			
Stress strain relationship & cylindrical compressive strength	–	Ø100 × 200 mm (NWC&LWC) Ø75 × 150 mm (ULCC)		28 days	
Static Young's modulus & Poisson's ratio	BS1881 −121:1983				
Flexural tensile strength	ASTM C 1609 M-05	102 × 76 × 402 mm			
Moisture content	RILEM CPC 11.3: 1984	Ø100 × 50 mm (NWC&LWC) 102 × 76 × 60 mm (ULCC)			

2.2.1. Tests under ambient temperature of about 30 °C

2.2.1.1. Density and compressive test. The density, compressive strength, elastic modulus, and Poisson's ratio of the concretes were determined according to relevant standards as given in Table 2. For each cylinder specimen, three strain gauges were used to measure axial strain and two strain gauges were used to measure transverse strain. At the same time, the axial deformations of the cylinder specimen were also measured by three linear variable displacement transducers (LVDTs). The load was applied at a constant displacement rate of 0.1 mm/min by using an automated computer controlled system throughout the tests. The load and deformation (from LVDTs) of the specimens were recorded continuously, and the modulus of elasticity and cylindrical compressive strength were obtained. The Poisson's ratio was calculated based on the axial and the transverse strains obtained from the strain gauges.

2.2.1.2. Flexural tensile test. Flexural performance of the 102 × 76 x 402-mm prisms was determined at 28 days with third-point loading (4-point bending, span length 300 mm) using an Instron closed-loop, servo-controlled testing system (Fig. 2) according to [3]. Load was applied at a constant deflection rate of 0.1 mm/min. During the test, both applied load and mid-span deflection of the specimen in the direction of the applied load were recorded. The deflection was measured by two LVDTs placed on both sides of the specimen. The load-deflection curve was obtained and the flexural performance parameters were derived using absolute values of the load or strength at specific deflections. The following parameters were obtained or calculated according to ASTM C1609:

L = Span length (300 mm in this case)
δ_P = Net deflection at Peak Load (mm)
f_p = Peak strength (MPa)
f_{600} = Residual Strength at net deflection of L/600 (0.5 mm)
f_{150} = Residual Strength at net deflection of L/150 (2 mm)
$Tough_{L/600}$ = Area under the load vs. net deflection curve 0 to L/600 (N·m)
$Tough_{L/150}$ = Area under the load vs. net deflection curve 0 to L/150 (N·m)

2.2.2. Tests at low temperatures from 0 to −60 °C

An MTS series 651 environmental chamber[1] attached to a MTS hydraulic testing machine was used for the concrete testing at the low temperatures of 0, -30, and −60 °C with the introduction of liquid nitrogen. Before each test, the specimen was cooled down to a specified testing temperature at a constant cooling rate of 1 K/min. The liquid nitrogen is injected into the chamber and distributed by a propeller according to the temperature controller. The temperature of the specimen was measured by two thermocouples, one mounted on the surface of the test specimen and the other embedded in the core of a reference specimen equivalent to the testing specimen. Once the specified testing temperature was reached inside the chamber, it was held constant for 30 min to make sure that the required temperature was achieved in the core of the specimen and stabilized with uniform temperature attained in the specimen. Test methods were the same as those described above.

2.2.3. Water accessible porosity and moisture content

As the performance of concrete at low temperatures is affected by the formation of ice in concrete pore system, the water accessible porosity of concrete is an important parameter. The water accessible porosity was determined by a water saturation method similar to that described in RILEM CPC 11.3 [10]. Three specimens of 102 × 76 × 60-mm cut from a 102 × 76 × 402-mm prism were used for the test of the ULCC and three specimens of Ø100 × 50-mm cut from a Ø100 × 200-mm were used for the NWC and LWC. From the mass of the specimen oven dried at 105 °C and the mass of a 'saturated surface dry' specimen determined in air and in water, the water accessible porosity (in volume of the concrete) was calculated as follows.

$$P_w = \frac{(m_s - m_o)/\rho}{(m_s - m_a)/\rho} \times 100\% \quad (3)$$

where m_a = apparent mass of the saturated specimen immersed in water (kg), m_o = oven dry mass of the specimen in air (kg), m_s = 'saturated surface-dry mass' of the specimen in air (kg), and ρ = density of water, ~1000 kg/m^3.

With the oven dry mass of the specimen, the moisture content of ULCC can also be obtained.

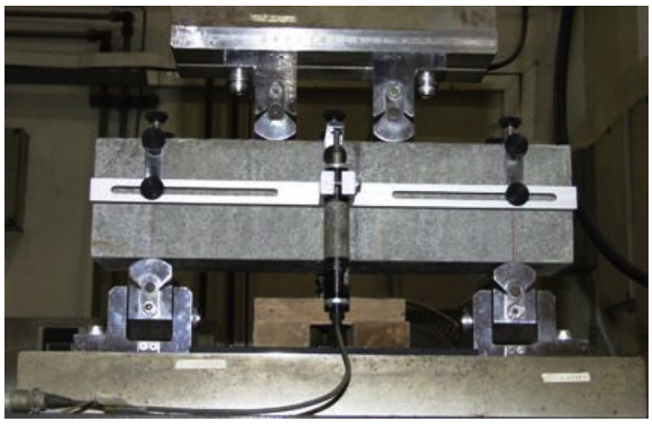

Fig. 2. Flexural test set-up.

3. Results and discussion

3.1. Workability, density, and compressive strength at ambient temperature of 30 °C

The workability, densities, and compressive strengths of the concrete cubes, f_{cu}, are given in Table 3. The ULCC had flow consistency of about 320 mm and was pumpable. The slump of the NWC and LWC was 130 mm.

The ULCC had 28-day density of approximately 1450 kg/m^3, about 40% and 25% lower than that of the NWC (2365 kg/m^3) and LWC (1915 kg/m^3), respectively. The ULCC(S) specimens moist cured for 28 days had slightly higher density (1–2%) than those of the ULCC(D) moist cured for 7 days. The ULCC had 28-day compressive strength of approximately 58 MPa regardless of the curing conditions. The NWC and LWC both achieved comparable compressive strength to that of the ULCC at 28 days.

3.2. Effect of curing condition on behavior of ULCC under low temperatures of 0 to −60 °C

3.2.1. Behavior under compressive loading

Stress-strain curves of the ULCC under different curing conditions are shown in Fig. 3. As it is well known that the role played by shape and slenderness of the concrete specimen is a function of temperature [4,12], cylinder specimens with the same aspect ratio were used to investigate the mechanical properties of the mixtures

[1] www.mts.com.

Table 3
Workability, density, and cube compressive strength of the concretes at ambient temperature of 30 °C.

	Curing	Flow table value, mm	Slump, mm	Density, kg/m^3				Cube compressive strength, f_{cu}, MPa	
				Demold	7 days	28 days	Oven-dry	7 days	28 days
ULCC (S)	28-d moist curing	325	–	1445	1455	1460	1305	51.4	58.6
ULCC (D)	7-d moist curing +21-d in lab air	320	–	1430	1440	1430	1295	49.8	57.4
NWC	7-d moist curing +21-d in lab air	–	130	2380	2390	2365	2260	55.6	68.4
LWC		–	130	1920	1930	1915	1790	50.8	55.3

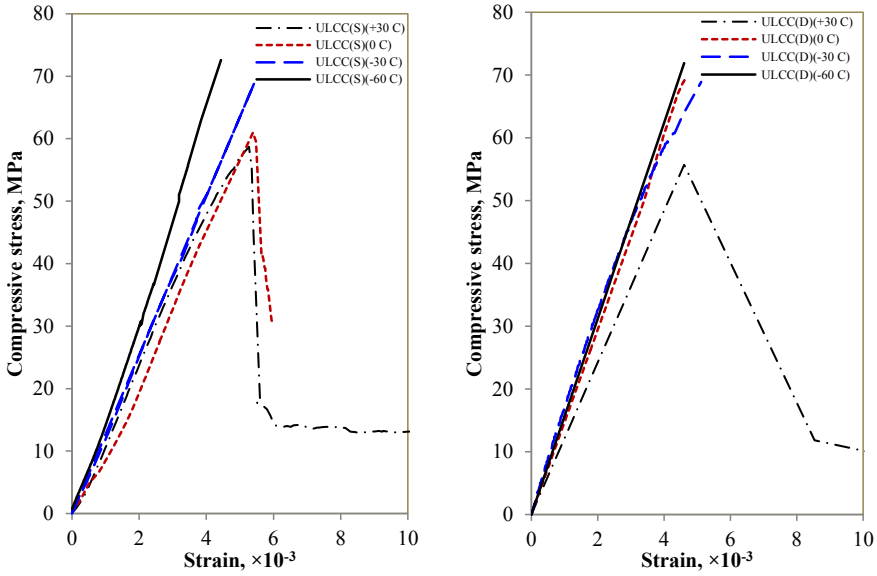

Fig. 3. Stress-strain curves of the ULCC with different curing conditions under various temperatures.

under different temperatures. The cylindrical compressive strengths (f_c), elastic modulus, Poisson's ratio, and strain at peak load of the cylinder specimens are calculated and presented in Table 4.

With different curing conditions, the cylindrical compressive strength, elastic modulus, Poisson's ratio and compressive strains of ULCC were not significantly different. As the hollow cenospheres were not filled with water, the strengthening effect at low temperatures $\leq$ 0 °C was due primarily to that of the cement paste matrix as water freezes. Due to the low w/b of 0.35 and 5% silica fume used in the ULCC, water may not be able to penetrate into the ULCC easily after initial moisture curing of 7 days. Thus, the moisture content of the ULCC(S) would not be significantly different from that of the ULCC(D) at the time of testing. The strength threshold of the cenospheres might have limited the compressive strength of the ULCC when the temperature dropped below freezing point of water. This may also explain the similar performance of the ULCC with different curing conditions.

The strain of the ULCC(S) at the peak load decreased by about 20% when the temperature was decreased to −60 °C although the strain at peak load was not affected by the temperatures from +30 °C to −30 °C. This corresponds well with the trend in the E-modulus, as the strain is related to E-modulus.

3.2.2. Behavior under bending

The 28-day flexural behavior of the ULCC cured under different conditions is illustrated in Fig. 4, and quantitative information obtained is given in Table 5. Effect of the curing conditions on the flexural toughness of the ULCC is presented in Fig. 5.

Both ULCC(S), moist cured for 28 days, and ULCC(D), moist cured

Table 4
Effect of curing conditions on cylindrical compressive strength (f_c), elastic modulus, Poisson's ratio, and strain at peak load of the cylinder ULCC at temperatures of 30 °C to −60 °C.

	Cylindrical compressive strength (SD), f_c, MPa				Elastic modulus (SD), GPa			
	30 °C	0 °C	−30 °C	−60 °C	30 °C	0 °C	−30 °C	−60 °C
ULCC(S)	58.6(0.7)	61.5(5.6)	66.8(3.4)	72.1(1.1)	13.1(0.1)	12.9(1.8)	13.3(0.9)	15.8(1.4)
ULCC(D)	55.7(1.5)	67.3(2.0)	67.5(3.5)	71.9(0.9)	14.0(3.1)	14.7(1.4)	15.7(1.1)	15.6(1.3)
	Poisson's ratio (SD)				Strain at peak load (SD), x 10^{-3}			
	30 °C	0 °C	−30 °C	−60 °C	30 °C	0 °C	−30 °C	−60 °C
ULCC(S)	0.23(0.02)	0.24(0.01)	0.22(0.01)	0.21(0.03)	5.3(0.1)	5.4(0.3)	5.4(0.4)	4.4(0.6)
ULCC(D)	0.24(0.02)	0.23(0.04)	0.21(0.01)	0.19(0.03)	4.6(0.6)	4.6(0.2)	4.5(0.3)	4.6(0.3)

Note: SD denotes standard deviation.

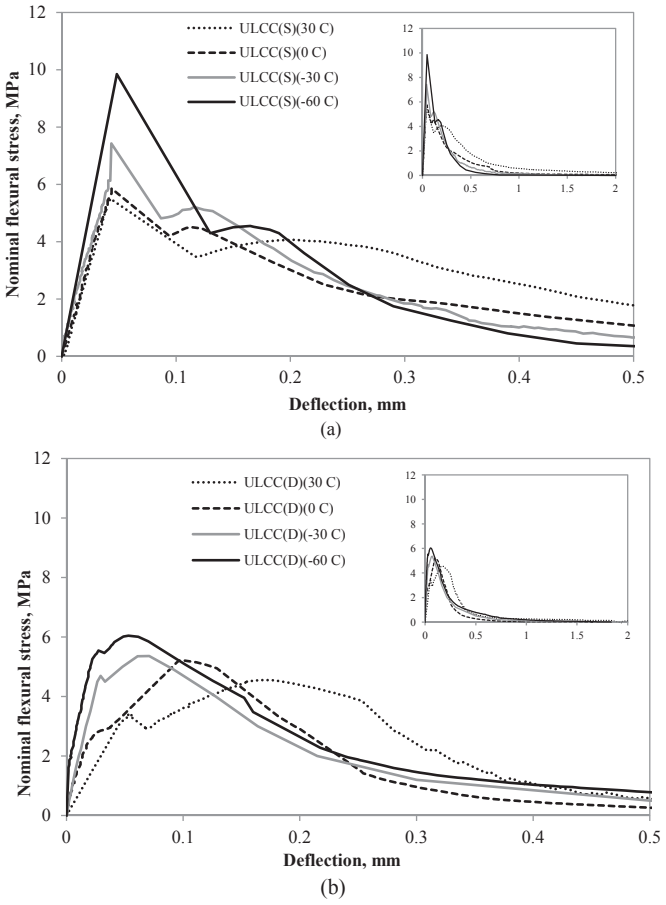

Fig. 4. Stress-deflection curves of (a) ULCC(S) and (b) ULCC(D) at various temperatures (insert shows deflection to 2 mm).

for 7 days, are characterized by a deflection-softening branch from the ambient temperature down to −60 °C (Fig. 4). The flexural strength of the ULCC was generally increased with the reduction in the temperature regardless of the curing conditions. However, the flexural strength of the ULCC(S) was about 25–38% higher than that of the ULCC(D) at various testing temperatures. It indicates that the curing condition has significant influence on the flexural strength of ULCC and the extension of the moisture curing days can improve the flexural strength. The different curing conditions did not affect the compressive strength significantly, on the contrary. One of the reasons of the lower flexural strength of the ULCC(D) was probably due to the drying shrinkage effect. When the ULCC(D) was exposed to laboratory air after an initial moist curing of 7 days, drying would cause non-uniform moisture distribution in the specimens, which might have resulted in drying shrinkage cracks near the concrete surfaces, and resulted in lower flexural strength. The strains at the

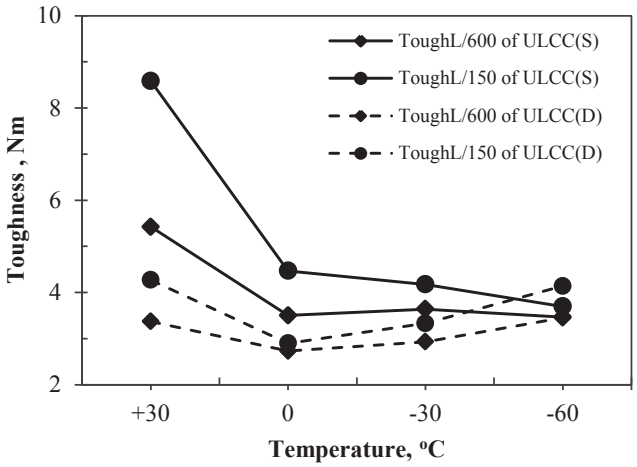

Fig. 5. Influence of curing conditions on toughness at different temperatures.

peak load of the ULCC(D) were higher than that of the ULCC(S), especially at 0 and 30 °C.

Residual strength f_{600} of the ULCC(D) which corresponded to mid-span deflection of 0.5 mm (L/600) was generally lower than that of the ULCC(S) except at the low temperature of −60 °C. The residual strength of the ULCC provided by the fibers represents the load-carrying capability of a cracked prism specimen. The residual strength f_{600} of the ULCC was reduced with the reduction in testing temperature, indicating that the ULCC became more brittle at low temperatures. The residual strength f_{150} which corresponded to mid-span deflection of 2 mm (L/150) was close to zero.

As shown in Fig. 5, the flexural toughness of the ULCC was generally not affected by the testing temperatures significantly except for the ULCC(S) with the temperature drop from 30 to 0 °C. At these temperatures, the flexural toughness of the ULCC(S) was reduced by about 35% and 48% at the deflections of 0.5 mm and 2.0 mm, respectively. The data presented in Table 5 indicate that the curing conditions had a noticeable effect on the toughness of the ULCC. The ULCC(S) generally had higher toughness than the ULCC(D), both at the deflections of 0.5 mm and 2 mm, except at −60 °C. The higher toughness of the ULCC(S) was related to its higher flexural tensile strength discussed earlier.

3.3. Performance of the ULCC in comparison to NWC and LWC at low temperatures

3.3.1. Behavior under uniaxial compressive loading

Stress-strain curves of the ULCC(D), NWC, and LWC at various temperatures are shown in Fig. 6 (a), (b), and (c), respectively. Cylindrical compressive strength (f_c), elastic modulus, Poisson's ratio, and strain at peak load of the concretes are summarized in Table 6.

When testing ULCC(D) at the ambient temperature of 30 °C, both ascending and descending portions of the stress-strain curve

Table 5
Flexural performance of the ULCC under different curing conditions.

	Unit	ULCC(S)				ULCC(D)			
		30 °C	0 °C	−30 °C	−60 °C	30 °C	0 °C	−30 °C	−60 °C
fp (standard deviation)	MPa	6.08 (0.81)	6.14 (0.34)	7.43 (1.15)	9.78 (1.06)	4.17 (0.35)	4.62 (0.52)	5.35 (0.12)	6.06 (0.16)
δp	mm	0.04	0.03	0.05	0.05	0.16	0.21	0.07	0.06
f_{600} (0.5 mm)	MPa	2.58	1.07	0.66	0.36	0.72	0.68	0.50	0.78
f_{150} (2.0 mm)	MPa	0.00	0.07	0.00	0.00	0.08	0.00	0.00	0.00
Toughness$_{L/600}$ (0.5 mm)	Nm	5.42	3.50	3.64	3.47	3.37	2.73	2.93	3.45
Toughness$_{L/150}$ (2.0 mm)	Nm	8.58	4.47	4.17	3.70	4.27	2.90	3.33	4.14

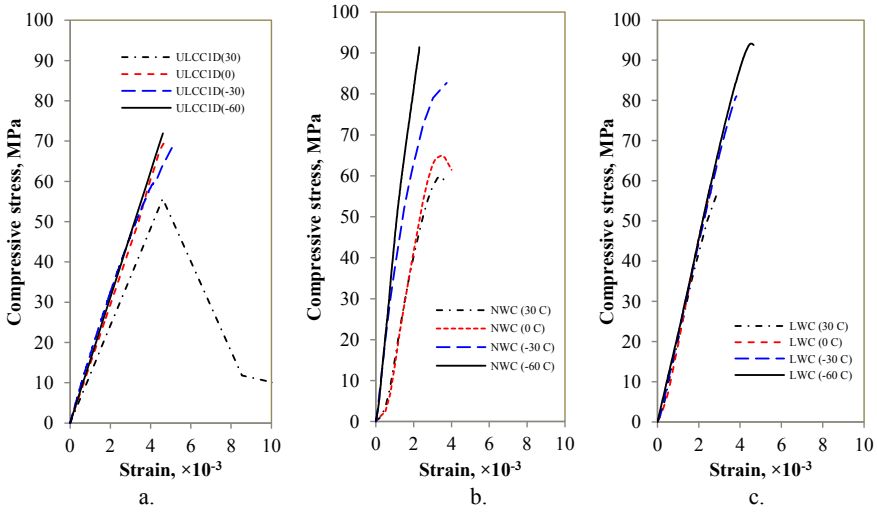

Fig. 6. Stress-strain diagrams of the concretes at the reference temperatures, (a) ULCCD; (b) NWC; (c) LWC.

Table 6
Compressive strength (f_c), elastic modulus, Poisson's ratio, and strain at peak load of the ULCC at temperatures of 30 °C to −60 °C in comparison to NWC and LWC.

	Cylindrical compressive strength[a] (SD), f_c, MPa				Elastic modulus (SD), GPa			
	30 °C	0 °C	−30 °C	−60 °C	30 °C	0 °C	−30 °C	−60 °C
ULCC(D)	55.7(1.5)	67.3(2.0)	67.5(3.5)	71.9(0.9)	14.0(3.1)	14.7(1.4)	15.7(1.1)	15.6(1.3)
NWC	60.0(1.7)	66.0(5.1)	82.4(7.0)	>92.0[b]	27.8(1.8)	28.7(2.1)	37.6(4.2)	45.4(3.6)
LWC	57.0(1.4)	57.1(2.0)	80.3(0.8)	90.7(3.2)	23.7(2.5)	24.7(1.1)	23.7(2.8)	23.5(0.9)
	Poisson's ratio (SD)				Strain at peak load (SD), $\times 10^{-3}$			
	30 °C	0 °C	−30 °C	−60 °C	30 °C	0 °C	−30 °C	−60 °C
ULCC(D)	0.24(0.02)	0.23(0.04)	0.21(0.01)	0.19(0.03)	4.6(0.6)	4.6(0.2)	4.5(0.3)	4.6(0.3)
NWC	0.20(0.03)	0.20(0.01)	0.21(0.01)	0.19(0.03)	3.2 (0.4)	2.8(0.9)	2.0(0.4)	>2.3[b]
LWC	0.19(0)	0.19(0.01)	0.18(0.01)	0.20(0.02)	2.9 (0.4)	2.6 (0.1)	3.8(0.4)	4.5(0.5)

SD denotes standard deviation.
[a] Directly obtained from the tests.
[b] NWC did not fail at this value due to the equipment loading capacity.

were obtained due to the incorporation of fibers. For the ULCC(D), ascending portion of the stress-strain curves was almost linear up to failure. However, no descending branch was obtained at lower temperatures. This may be attributed to the formation of ice in capillary pores, which resulted in a more brittle behavior of the ULCC at lower temperatures.

For the NWC, the stress-strain curves were not linear except for the one obtained at −60 °C. Non-linearity of the curves is related to microcrack propagation at interface transition zone (ITZ) between coarse aggregate and mortar matrix. Stress-strain curves of the LWC were almost linear. No descending portion of the stress-strain curves was obtained for the NWC and LWC because no fibers were used in these two concretes.

As shown in Fig. 7, cylindrical compressive strength, f_c, of the ULCC(D), NWC, and LWC increased generally with the reduction in temperature. The strength increase of the LWC was similar to that of the NWC. However, strength increase of the ULCC(D) was less than that of the NWC and LWC as temperature decreased to −60 °C. The stronger paste with ice formation at the low temperatures probably contributed to the strength increase. The hollow cenospheres are generally not penetrable by water unless the cenospheres are broken which might not happen in most cases. Thus, the strength of the cenospheres might not increase with the reduction in the temperatures below 0 °C. The LWA used in LWC, however, was pre-soaked and would become stronger at the low

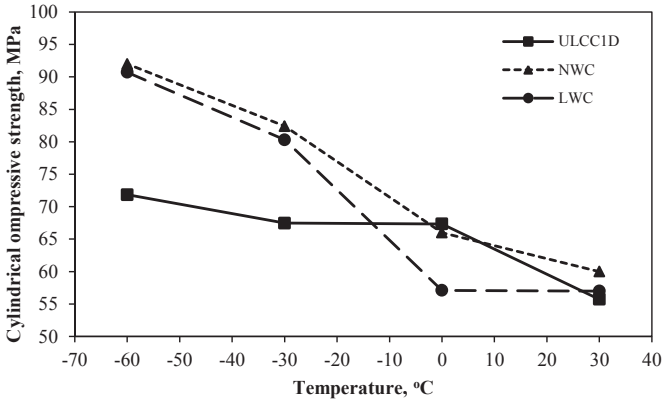

Fig. 7. Cylindrical compressive strength of ULCC (D), f_c, under different temperatures in comparison to that of the NWC and LWC.

temperatures due to the formation of ice. This resulted in greater strength increase of the LWC at the low temperatures. Thus, the strength increase of the ULCC at the low temperatures might be attributed primarily to the stronger paste, whereas the strength increase of the LWC might be attributed to the stronger paste and stronger LWA [33]. also reported increased cylindrical strength of LWC with reduced temperature below zero. It should be noted that

the NWC did not fail when tested at −60 °C due to the loading capacity of the testing equipment. The strength of the ULCC(D) at −60 °C was about 1.3 times of that at the ambient temperature, whereas strength of the LWC and NWC was 1.6 and > 1.5 times of that at the ambient temperature at 30 °C, respectively. This may be related to pore structure of the concretes.

Water accessible porosity and moisture content of the concretes at the time of testing are given in Table 7. The water accessible porosity is considered an important parameter which reflects porosity, interface transition zone between the aggregate and cement paste matrix, and microcracks in the concrete, and has significant influence on the permeability of hardened concrete [22]. The moisture content has been identified as a key parameter that influences the strength increase of conventional concrete under sub-zero temperatures. The less strength increase of the ULCC(D) observed at the lower temperatures might be attributed to the "strength ceiling" effect of the hollow cenospheres. The moisture content of the ULCC, therefore, might not be as critical as for the conventional NWC and LWC.

The ULCC(D) had significantly lower elastic modulus than the NWC and LWC. The elastic modulus of the ULCC(D) increased slightly from 14.0 to 15.6 GPa whereas that of the NWC increased significantly from 27.8 to 45.3 GPa with the temperature drop from 30 °C to −60 °C. The increase in the elastic modulus of the NWC with the reduction of temperature is consistent with the findings by Ref. [31]. This might be related to strengthened paste matrix and especially the ITZ between the aggregate and the matrix due to the formation of ice. The improved ITZ resulted in more linear stress-strain curves and less damage in the ITZ. The elastic modulus of the LWC was not affected by the temperature from 30 °C down to −60 °C. This may be explained partly by difference of the microstructure between LWC and NWC. Due to water absorption of the LWA, the interface zone between LWA and cement paste is usually denser than that between the NWA and paste. Thus, freezing at low temperatures may not have significant effect on the ITZ in the LWC as in the NWC. Although the formation of ice increased the strength of the LWC, it did not affect its elastic modulus. Further investigation is needed on the observed independence of the LWC elastic modulus with the temperatures.

Based on statistical analyses at a confidence level of 95%, Poisson's ratio of the ULCC(D) was constant from ambient temperature of about 30 °C to 0 °C, but decreased with further temperature reduction to −30 °C and −60 °C. The Poisson's ratios of the NWC and LWC were not affected by the reduction of the temperatures. Limited information on the Poisson's ratio of normal weight concrete at various sub-zero temperatures is available with contradictory findings. Ref. [30] reported that Poisson's ratio is not affected by temperature in a range from 24 °C to −157 °C, whereas [31] reported that the Poisson's ratio increases from about 0.17 at 20 °C to 0.22 at −165 °C for normal weight concrete.

Due to the lower elastic modulus, the strain at the peak load of the ULCC(D) was generally much higher than that of NWC and LWC, and was generally not affected by the temperature. However, no consistent trend of the strain at the peak load vs temperature was observed for the LWC and NWC.

Table 7
Water accessible porosity of the ULCC, LWC, and NWC.

	Water accessible porosity, % volume	Moisture content, (*W*) %
ULCC(S)	16.1	12.1
ULCC(D)	15.6	11.4
NWC	12.0	5.1
LWC	11.7	6.5

3.3.2. Behavior under bending

The ULCC is less brittle than the LWC and NWC due to the incorporation of fibers. When subjected to bending, load-deflection curves of the NWC and LWC only had ascending portion up to the peak load. For the ULCC(D), however, descending portion of the load-deflection curve was also obtained at ambient temperature and was discussed in previous section.

Fig. 8 shows effect of temperature on the flexural strength of the concretes, and it is clear that the flexural strength was increased when temperatures dropped from 30 °C to −60 °C. At various temperatures, the ULCC and LWC had comparable flexural tensile strengths which were much lower than those of the NWC. The lower tensile strength of the LWC than NWC with comparable compressive strength was reported by Ref. [7]; and the same phenomenon was observed for the ULCC. At −60 °C flexural strength of the ULCC(D), LWC, and NWC was 1.5, 1.7, and 1.6 times that at the ambient temperature of 30 °C, respectively. The increasing trend in the flexural strength with the temperature reduction is consistent with the findings by Refs. [21] and [37] on splitting tensile strength of NWC. Experimental results also show that the percentage increase in the flexural strength of the NWC was similar to that of the compressive strength when the temperature dropped from 30 °C to − 60 °C. This was consistent with previous finding by Ref. [21].

3.4. Compressive strength at low temperatures

For NWC the strength increase has been found to be nearly proportional to the moisture content, regardless of the curing – wet, air dried, or oven dried. The compressive strength of NWC at very low temperature can be expressed as:

$$f_{CL} = f_{CO} + \Delta f_C \tag{4}$$

Δf_C is nearly proportional to the moisture content of concrete (W), where f_{CL} is the compressive strength of the concrete at very low temperature, f_{CO} is the compressive strength of the concrete at normal temperature, and Δf_C is the increase of the compressive strength of concrete at very low temperature. Ref. [29] suggested Eqs (5) and (6) to calculate the strength increase of NWC at very low temperatures.

$$\Delta f_C = \left\{12 - \frac{1}{2700}(T+180)^2\right\} \cdot W, \mathrm{N/mm^2} \quad T \geq -120^{o}\mathrm{C} \tag{5}$$

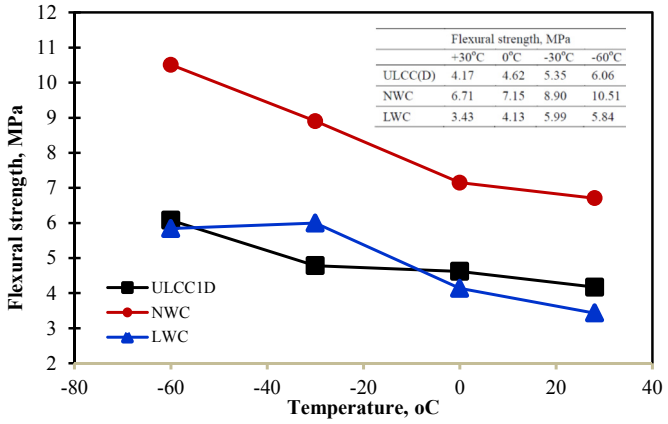

Fig. 8. Flexural strength of ULCCD at low temperatures relative to those of NWC and LWC.

$$\Delta f_C = 10.7 \cdot W, \mathrm{N/mm^2} \quad T < -120^{o}\mathrm{C} \tag{6}$$

where T is temperature (°C), W is moisture content (%, by wt).

The strength of NWC in this study and the estimated strength by Eq. (5) are presented in Fig. 9. It indicates that Miura's equation provides a reliable prediction on the compressive strength of the NWC with prediction errors less than 9%. The strength of the LWC in this study was presented in Fig. 9 as well in comparison to that estimated using the same equation. It was found that the compressive strength of the LWC under very low temperatures can also be predicted by Miura's equation, and the strength increase of the LWC was greater than that of the NWC due to higher moisture content of the former. This finding is opposite to that by Ref. [24]. The difference might be attributed to the strength of LWC relative to its "strength ceiling". If the strength of a LWC is far below its strength ceiling, the strength increase of the LWC may be greater than that of NWC due to higher porosity and moisture content of the LWC. However, if the strength of a LWC is close to its strength ceiling, the strength increase of the LWC at subzero temperatures may be limited and less than that of NWC. The ULCC in this study may be an example, and their strengths were not increased significantly when the temperature dropped from 0 down to −60 °C (Fig. 10). Miura's equation does not seem to be applicable to the ULCC. For design purpose, the compressive strength of the ULCC under subzero temperatures may be conservatively estimated by using its compressive strengths at ambient temperature of 30 °C or at 0 °C.

4. Conclusions

Compressive and flexural behavior of the ULCC under low temperatures of 0 °C, -30 °C, and −60 °C are investigated in comparison to those at an ambient temperature of about 30 °C. Effect of moist curing of 7 and 28 days on its mechanical performance is also evaluated. The results are also compared with those of a NWC and a LWC with similar 28-day compressive strength. Based on experimental results, following conclusions can be drawn:

- The stress-strain curves of the ULCC and LWC were almost linear in the ascending branch, whereas those of the NWC were not linear except for the one obtained at −60 °C.
- Compressive strength of the NWC and LWC increased generally with the reduction in temperature. However, the same phenomenon was not observed for the ULCC. This might be due to the "strength limit" of the cenospheres. For design purpose, therefore, the compressive strength of the ULCC under subzero temperatures may be conservatively estimated by using its compressive strengths at ambient temperature of 30 °C or at 0 °C.
- The ULCC had significantly lower elastic modulus than the NWC and LWC. The elastic modulus of the ULCC(D) increased slightly from 14.0 to 15.6 GPa whereas that of the NWC increased significantly from 27.8 to 45.3 GPa with reduction of temperature from 30 °C to −60 °C. The elastic modulus of the LWC was not affected by the temperature significantly in the same range.
- Strain at the peak load of the ULCC was generally much higher than that of the NWC and LWC, and was generally not affected by the temperature. No consistent trend of the strain at the peak load vs temperature was observed for the LWC and NWC.
- Poisson's ratio of the ULCC was not changed with temperature drop from 30 to 0 °C, but was decreased with further temperature reduction to −30 and −60 °C. The Poisson's ratios of the NWC and LWC were not affected by the reduction in the temperatures.
- The flexural strength of the three concretes was increased with the reduction in temperature. At various temperatures, the ULCC and LWC had comparable flexural tensile strengths which were much lower than those of the NWC.
- Moist curing durations of 7 and 28 days did not affect the performance of the ULCC under compressive loading significantly. However, the flexural strength of the ULCC moist cured for 28 days was about 25–38% higher than that of the ULCC moist cured for 7 days and dried for 21 days in lab air, possibly due to drying shrinkage effect on specimen surface.

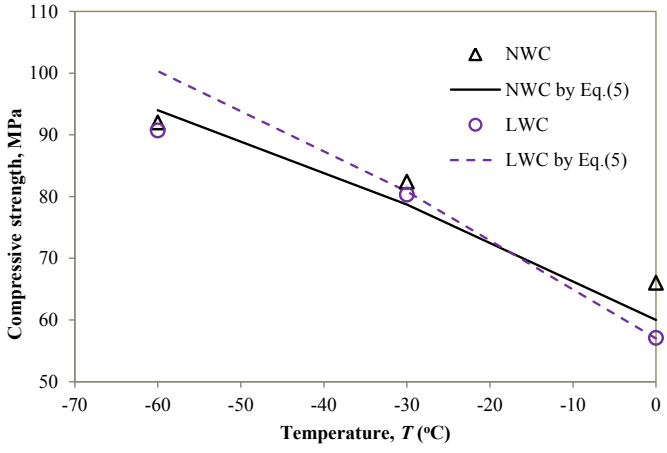

Fig. 9. Compressive strength of NWC and LWC in comparison to the strength estimation by Eq. (5).

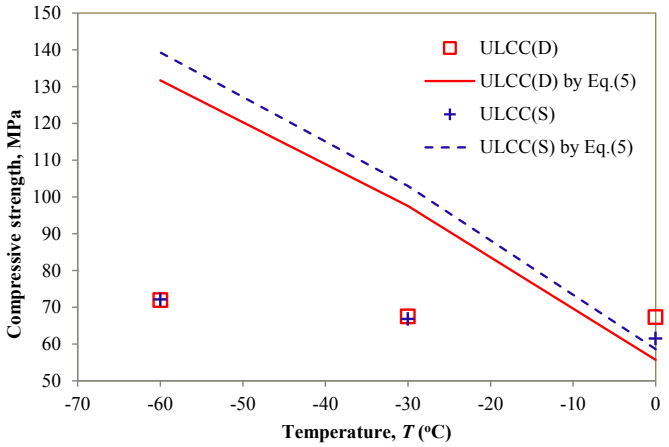

Fig. 10. Compressive strength of ULCC in comparison to the estimated strength by Eq. (5).

Acknowledgments

Grateful acknowledgement is made to A*Star, Science and Engineering Research Council of Singapore (Project no. 0921420044) for funding this research.

References

[3] ASTM C1609/C1609M-07, Standard Test Method for Flexural Performance of Fiber-reinforced Concrete (Using Beam with Third-point Loading), American Society of Testing and Materials, 2007.
[4] P. Bamonte, P.G. Gambarova, Thermal and mechanical properties at high temperature of a very high-strength durable concrete, ASCE J. Mater. Civ. Eng.

22 (6) (2010) 545–555.
[5] BS EN 197–1, Cement. Composition, Specifications and Conformity Criteria for Common Cements, 2011.
[7] R.L. Carrasquillo, A.H. Nilson, F.O. Slate, Properties of high strength concrete subject to short-term loads, ACI J. Proc. 78 (3) (May-June 1981) 171–178.
[8] R.J. Cardoso, A. Shukala, A. Bose, Effect of particle size and surface treatment on constitutive properties of polyester-cenosphere composites, J. Mater. Sci. 37 (2002) 603–613.
[9] K.S. Chia, M.-H. Zhang, J.Y. Liew, High-strength ultra lightweight cement composite -material properties, in: Ninth International High Performance Concrete Symposium, Rotorua, New Zealand, August, 2011, pp. 9–11.
[10] CPC11.3, Absorption of water by concrete by immersion under vacuum, in: E, FN SPON (Eds.), RILEM Recommendations for the Testing and Use of Constructions Materials, RILEM, 1984.
[11] R.L. Day, Strength measurement of concrete using different cylinder sizes: a statistical analysis, Cement, Concrete, and Aggregates, CCAGPD 16 (1) (1994) 21–30.
[12] M. Di Prisco, R. Felicetti, P.G. Gambarova, C. Failla, in: On the Fire Behavior of SFRC and SFRC Structures in Tension and Bending, Proceeding of 4th International Workshop on High-performance Fiber-reinforced Cement Composites HPFRCC-4, 2003, pp. 205–220. Ann Arbor (Michigan, USA).
[13] Dmi, Arctic Temperatures – Daily Mean Temperatures North of 80 Degree North, Dmi Centre for Ocean and Ice, 2014. http://ocean.dmi.dk/arctic/meant80n.uk.php.
[16] R.A. Helmuth, Capillary size restrictions on ice formation in hardened Portland cement pastes, in: Fourth International Symposium on the Chemistry of Cement, Washington, 1960, pp. 855–869.
[18] M.C. Juenger, C.P. Ostertag, Alkali–silica reactivity of large silica fume-derived particles, Cem. Concr. Res. 34 (2004) 1389–1402.
[21] G.C. Lee, T.S. Shih, K.C. Chang, Mechanical properties of concrete at low temperatures, J. Cold Regions Eng. 2 (1) (1988) 13–24.
[22] X. Liu, K.S. Chia, M.-H. Zhang, Development of lightweight concrete with high resistance to water and chloride-ion penetration, Cem. Concr. Compos. 32 (2010) 757–766.
[23] X. Liu, K.S. Chia, M.-H. Zhang, J.Y. Liew, Water and chloride ion penetration resistance of high strength ultra lightweight cement composite, Int. Congr. Durab. Concr. Trondheim, Nor. June (2012) 18–21.
[24] A.L. Marshal, Cryogenic Concrete, Cryogenics, Butterworth & Co (Publishers) Ltd., 1982, pp. 555–565.
[25] A.J. Maas, J.H. Ideker, M.C. Juenger, Alkali silica reactivity of agglomerated silica fume, Cem. Concr. Res. 37 (2007) 166–174.
[27] K.W. Nasser, G.A. Evans, Low temperature effects on hardened air entrained concrete. Behavior of concrete under temperature extremes, ACI SP-39 (1973) 79–90.
[28] S. Mindess, J.F. Young, D. Darwin, Concrete, second ed., Prentice Hall, Upper Saddle River, NJ, 2003.
[29] T. Miura, The properties of concrete at very low temperatures, Mater. Struct. 22 (1989) 243–254.
[30] G.E. Monfore, A.E. Lentz, Physical properties of concrete at very low temperatures, J. Portland Cem. Assoc. R&D Lab Bull (1962) 33–39.
[31] T. Okada, M. Iguro, Bending behavior of prestressed concrete beams under low temperatures, J. Jpn. Prestress. Concr. Eng. Assoc. 20 (8) (1978) 15–17.
[33] F.S. Rostásy, U. Pusch, Stregnth and deformation of lightweight concrete of variable moisture content at very low temperatures, Int. J. Cem. Compos. Lightweight Concr. 9 (1) (1983) 3–17.
[34] F.S. Rostásy, G. Wiedemann, Stress-strain-behaviour of concrete at extremely low temperature, Cem. Concr. Res. 10 (1980) 565–572.
[35] A. Skapski, R. Billups, A. Rooney, Capillary cone method fordetermination of surface tension of solids, J. Chem. Phys. 26 (5) (1957) 1350–1351.
[36] J.Y. Wang, M.H. Zhang, W. Li, K.S. Chia, J.Y.R. Liew, Stability of cenospheres in lightweight cement composites in terms of alkali-silica reaction, Cem. Concr. Res. 42 (2012) 721–727.
[37] S. Yamane, H. Kasami, T. Okuno, in: Douglas McHenry (Ed.), Properties of Concrete at Very Low Temperatures, Proceedings of International Symposium on Concrete and Concrete Structures, SP-55, American Concrete Institute, 1978, pp. 207–221.